Distance Measurements Using Partial Donor−Donor Energy Migration within Pairs of Fluorescent Groups in Lipid Bilayers

Stanislav Kalinin, Julian G. Molotkovsky,† and Lennart B.-Å. Johansson*

Department of Chemistry, Biophysical Chemistry, Umeå University, S-901 87 Umeå, Sweden, and Shemyakin & Ovchinnikov Institute of Bioorganic Chemistry, Russian Academy of Sciences, Miklukho-Maklaya 16/10, 117988 Moscow, Russia

Received: December 31, 2002; In Final Form: February 11, 2003

For distance measurements the fluorescence relaxation was explored within pairwise interacting chemically identical, but photophysically different fluorescent groups. The recently developed theory (Kalinin, S. V.; et al. *Spectrochim. Acta, Part A* **2002**, *58*, 1087−1097) of partial donor−donor energy migration (PDDEM) was tested on lipid vesicles as a model system, which, for example, enables arrangement of a pH gradient between the inside and outside of the lipid bilayer. Time-correlated single-photon counting and steady-state fluorescence experiments were performed on mono- and bis-lipid derivatives of fluorescein solubilized in lipid bilayers. The PDDEM approach was successfully applied in the analyses of the different experiments. The distances extracted between the fluorescein groups of bis-fluorescein derivatives in lipid vesicles composed 1,2-dioleoyl-*sn*-glycero-3-phosphocholine and 1,2-dimyristoyl-*sn*-glycero-3-phosphocholine were found to be in reasonable agreement with independent measurements of the bilayer thickness.

Introduction

For detailed structural insights into biosystems, distances between well-defined positions are required. During the last 30 years fluorescence resonance energy transfer (FRET) was used for measuring distances.[1,2] One major limitation of this method is to achieve the *specific* incorporation of a donor and an acceptor group in biomacromolecules such as proteins. A recently developed method based on donor−donor energy migration (DDEM) circumvents this problem. The DDEM method was developed[3−5] and applied in studies of protein structure, in particular the serine protease inhibitory (Serpin) mechanism.[6,7] Contrary to the NMR and X-ray methods, the DDEM method measures long distances (i.e., multiples of 10 Å), thus compatible with the typical size of proteins and the thickness of lipid bilayers. Prior to applications on proteins systems, the DDEM method was stepwise developed and tested by means of on-purpose synthesized model systems,[3,8] as well as by means of proteins of known X-ray structure.[4,5] A major drawback with the DDEM method is the requirement of fluorescent groups that are relatively inert to the local polarity in their surrounding. For this, BODIPY[9,10] has proven to be a very useful candidate for DDEM measurements. The search for other fluorescent photophysically inert groups with other Förster radii ($R_0^{\mathrm{BODIPY}} = 57$ Å) is useful, although not a straightforward task.

The present work aims at showing that even chemically identical, but photophysically different, fluorophores can be useful for distance measurements, provided a relevant theory is available for the analyses of experimental data. A recently published paper describes in detail the theory of partial donor−donor energy migration (PDDEM).[11] Contrary to the DDEM method, for which fluorescence depolarization experiments are needed, it was shown that distance information is already available in the photophysics' decay of DD pairs being sensitive to their local environment.

Lipid bilayes are characterized by various methods, including fluorescence methods.[2,12−16] This study demonstrates that the PDDEM theory[11] is applicable for the analyses of distances in artificially prepared systems for which distances between the donor−donor groups are known. We have studied a lipid-spanning bifluorescein molecule in vesicles of different bilayer thickness as model systems. Depending on pH, the fluorescein (Fl) group exists in equilibrium dominated by the mono- (Fl^{1-}) and dianionic (Fl^{2-}) forms.[17,18] Because of spectral overlap between the different forms, partial energy migration takes place. For such a system trans-bilayer and pairwise PDDEM occurs between $Fl^{1-} \leftrightarrow Fl^{2-}$, while donor−donor energy migration (DDEM) occurs between $Fl^{1-} \leftrightarrow Fl^{1-}$ and $Fl^{2-} \leftrightarrow Fl^{2-}$. To obtain chemically different environments, pH gradients were created between inside (pH_{in}) and outside (pH_{out}) the vesicles. Because the concentration of Fl^{1-} and Fl^{2-} depend on pH, this adds more complexity to the analyses of data. Here the theory of PDDEM is shown also to account for this case, which further strengthens its validity.

Materials and Methods

1,2-Dimyristoyl-*sn*-glycero-3-phosphocholine (DMPC), 1,2-dioleoyl-*sn*-glycero-3-phosphocholine (DOPC), and 1-palmitoyl-*sn*-glycero-3-phosphocholine (lyso-PPC) were purchased from Avanti Polar Lipids (U.S.A.). 8-Hydroxypyrene-1,3,6-trisulfonic acid (pyranine) was purchased from Molecular Probes, Inc. (U.S.A.). The detailed syntheses of dotriacontanedioic acid bis-(fluoresceinyl-5-methylamide) ($FlC_{32}Fl$) and 5-(hexadecanoyl-aminomethyl) fluorescein (FlC_{16}) will be published elsewhere.[19] The syntheses are briefly given below.

* Corresponding author. E-mail: lennart.johansson@chem.umu.se. Telephone: +46-90-786 5149. Fax: +46-90-786 7779.
† Russian Academy of Sciences.

10.1021/jp022672c CCC: $25.00
Published on Web 03/19/2003

Syntheses of Dotriacontanedioic Acid Bis(fluoresceinyl-5-methylamide) ($FlC_{32}Fl$) and 5-(Hexadecanoylaminomethyl)fluorescein (FlC_{16}). Dotriacontanedioic acid (2.3 mg)[20] was transformed into activated ester by the action of (benzotriazol-1-yloxy)tris(dimethylamino)phosphonium hexafluorophosphate (BOP) reagent (Fluka), and 1-methylimidazole (Aldrich) in dichloromethane/THF mixture. The ester was treated with 5-(aminomethyl)fluorescein hydrochloride (Molecular Probes) (4.8 mg) and *N*-ethyldiisopropylamine in THF to give, after reversed-phase chromatography on LiChroprep RP18 (Merck) in methanol, $FlC_{32}Fl$ (red powder, 1.2 mg, 22%); ESI-MS, *m/z*: 1197.56 $[M]^+$; UV (5 mM Me_4NOH in methanol): 497 nm ($\epsilon = 1.4 \times 10^5\ M^{-1}\ cm^{-1}$).

5-(Aminomethyl)fluorescein hydrochloride (2 mg) was acylated with excess palmitoyl chloride and 1-methylimidazole in THF; after chromatography, as above, FlC_{16} was obtained (orange powder, 2.4 mg, 80%), MALDI-MS, *m/z*: 600 $[M]^+$; UV (5 mM Me_4NOH in MeOH): 497 nm ($\epsilon = 7.2 \times 10^4\ M^{-1}\ cm^{-1}$).

Vesicle Preparation. The vesicles were prepared by the extrusion method[21] using an extruder manufactured by Lipex Biomembranes Inc. (Vancouver, Canada). The lipids and the probes, dissolved in chloroform or ethanol, were mixed and dried by a flow of nitrogen. The lipid film thus obtained was dispersed in a buffer. We used phosphate (100 mM $[Na_2HPO_4 + NaH_2PO_4]$, pH 5.76−8.57), or HEPES buffers (10 mM HEPES, 50 mM Na_2SO_4, pH 7.5). The lipid dispersion was freeze−thawed five times and extruded 10 times through a stack of two Nucleopore filters with a pore-size diameter of 100 nm (Corning, U.S.A.). The final lipid concentration was 0.5 mg/mL, and the probe/lipid molar ratio was less than 1:4000.

The vesicles enclosing the pyranine dye were prepared in the same way, with the exception of initially using 1 mM pyranine in a HEPES buffer. Nontrapped pyranine was removed by passing the sample through a HiTrap desalting column (Pharmacia Biotech, Sweden) equilibrated with HEPES buffer. The complete procedure is described in the paper of Kamp and Hamilton.[22]

Absorption and Time-Resolved Fluorescence Measurements. Absorption spectra were recorded on a GBC 920 spectrophotometer (GBC, Australia). A PRA 3000 (PRA, Canada) and an IBH 5000U (IBH, Scotland) system were used for time-correlated single-photon-counting (TCSPC) measurements. The excitation sources were NanoLED-01 and NanoLED-05 (IBH, Scotland) pulse diodes, operated at ca. 800 kHz. The excitation and emission wavelengths were selected using IBH monochromators or interference filters or both (Melles Griot, The Netherlands) centered at 460, 500, and 550 nm. The fluorescence decays were collected over 1024 channels with the resolution of 50 ps/ch, with at least 10 000 photons in the peak maximum.

Steady-State Fluorescence Measurements were performed on an SPEX Fluorolog 3 instrument (Jobin Yvon Inc, U.S.A.). The spectral bandwidths were typically set to 2 and 5 nm for the excitation and emission monochromators, respectively. All spectra were corrected. The fluorescence quantum yields were measured by using a derivative of a perylene dye in chloroform as a reference.[23]

All the experiments were performed at 295 K unless stated otherwise. The maximum absorbance of all samples was kept below 0.08. The samples were thermostated within 1 K. pH was controlled using an In Lab 422 microelectrode (Mettler-Toledo, Switzerland).

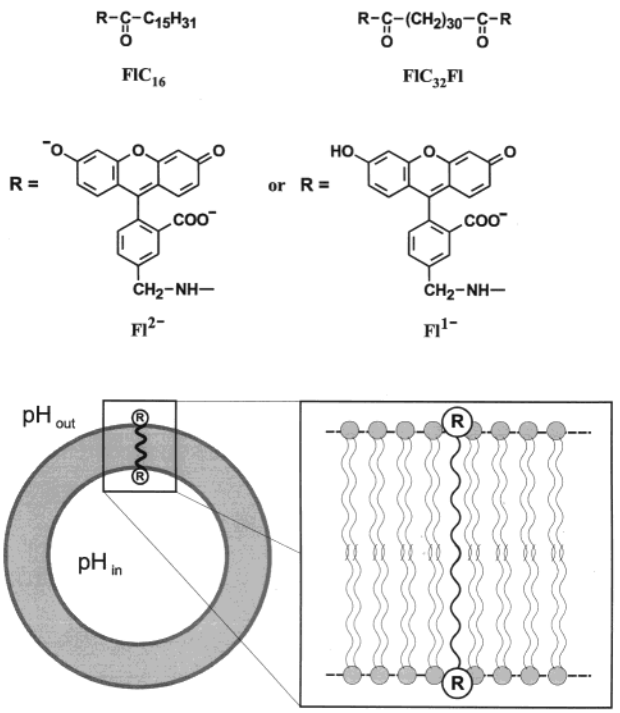

Figure 1. Chemical structures of dotriacontanedioic acid bis(fluoresceinyl-5-methylamide) FlC_{16} and 5-(hexadecanoylaminomethyl)fluorescein $FlC_{32}Fl$. The fluorescein chromophore exhibits as anionic (Fl^{1-}) or dianionic (Fl^{2-}) forms. A schematic of $FlC_{32}Fl$ molecule solubilized in lipid vesicle is also shown.

Generating Synthetic TCSPC Data. The synthetic TCSPC data was generated as described by Chowdhury et al.[24] and adapted to PDDEM in a previous work.[11] The generated data were analyzed in the same way as the experimental data.

Fluorescein Protolytic Reactions and Decomposition of the Spectra. The equilibria between different species of fluorescein (Fl) in aqueous media are rather complex.[12,17,18] In this work it was necessary to consider two fluorescent species (see Figure 1), namely, the dianion (Fl^{2-}) and the monoanion (Fl^{1-}).[17,18] These ionic forms exist at relatively high pH, and the following equilibria are relevant for the pH range studied (see the text below):

$$Fl \overset{K_1}{\rightleftharpoons} Fl^{1-} + H^+ \overset{K_2}{\rightleftharpoons} Fl^{2-} + 2H^+ \qquad (1)$$

It can be shown that the fractions of the components c_α and c_β (i.e. the ratios of $[Fl^{1-}]$ to the total concentration of fluorescein and $[Fl^{2-}]$ to the total concentration of fluorescein, respectively,) are given by

$$c_\alpha = (1 + [H^+]/K_1 + K_2/[H^+])^{-1}$$

$$c_\beta = (1 + [H^+]/K_2 + [H^+]^2/(K_1K_2))^{-1} \qquad (2)$$

The pK_1 and pK_2 values and the individual spectra of Fl^{2-} and Fl^{1-} were calculated from spectral data in a way similar to that which was described by Kubista and co-workers.[25] The pyranine spectra were analyzed in the same way with the exception that a single-step ionization model was used.[12] The individual spectra were also obtained from two-dimensional excitation−emission spectra with the use of the DATAN algorithm.[26]

Theoretical Prerequisites

Analyses of Time-Resolved Fluorescence Data. Previously, a complete description of the PDDEM model was presented.[11]

To summarize, a coupled system of two fluorophores D_α and D_β was considered, where in the present study the subscripts α and β refer also to the Fl^{1-} and Fl^{2-} forms, respectively (cf. Material and Methods). The lifetimes of D_α and D_β are denoted by τ_α and τ_β, and the rates of energy transfer from D_α to D_β and from D_β to D_α are $\omega_{\alpha\beta}$ and $\omega_{\beta\alpha}$, respectively. The fluorescence relaxation of a $D_\alpha-D_\beta$ system is given by

$$F_{\alpha\beta}(t) = \boldsymbol{p}_{ex}^t \boldsymbol{C}_1 \boldsymbol{p}_{em} \exp(\lambda_1 t) + \boldsymbol{p}_{ex}^t \boldsymbol{C}_2 \boldsymbol{p}_{em} \exp(\lambda_2 t) \quad (3)$$

In eq 3

$$\lambda_{1,2} = \frac{1}{2}[-1/\tau_\alpha - 1/\tau_\beta - \omega_{\alpha\beta} - \omega_{\beta\alpha} \pm \sqrt{(1/\tau_\alpha - 1/\tau_\beta + \omega_{\alpha\beta} - \omega_{\beta\alpha})^2 + 4\omega_{\alpha\beta}\omega_{\beta\alpha}}]$$

$$\boldsymbol{C}_{1,2} = \frac{1}{\lambda_1 - \lambda_2}\begin{pmatrix} \mp\lambda_{2,1} \mp 1/\tau_\alpha \mp \omega_{\alpha\beta} & \pm\omega_{\alpha\beta} \\ \pm\omega_{\beta\alpha} & \mp\lambda_{2,1} \mp 1/\tau_\beta \mp \omega_{\beta\alpha} \end{pmatrix} \quad (4)$$

and $\boldsymbol{p}_{ex}$ and $\boldsymbol{p}_{em}$ are the excitation and emission probabilities:[11]

$$\boldsymbol{p}_{ex} = \begin{pmatrix} p_{ex}^\alpha \\ p_{ex}^\beta \end{pmatrix}; \qquad \boldsymbol{p}_{em} = \begin{pmatrix} p_{em}^\alpha \\ p_{em}^\beta \end{pmatrix} \quad (5)$$

The rate of the energy transfer depends on the distance R between centers of mass of D_α and D_β, according to[27]

$$\omega = \frac{3\langle\kappa^2\rangle}{2\tau}\left(\frac{R_0}{R}\right)^6 \quad (6)$$

In eq 6, τ stands for the fluorescence lifetime of the donor, $\langle\kappa^2\rangle$ is the square of the angular part of dipole−dipole interaction, and R_0 is the Förster radius. The latter is defined by

$$R_0 = \left(\frac{9000 \ln 10(^2/_3)\Phi J}{128\pi^5 n^4 N_A}\right)^{1/6} \quad (7)$$

In eq 7 N_A, n, Φ, and J denote the Avogadro constant, the refractive index, the quantum yield of the donor, and the overlap integral, respectively.

If the fluorescence relaxation of D_α and D_β is nonexponential and described by

$$F_\alpha(t) = \sum_i f_\alpha^i \exp(-t/\tau_\alpha^i)$$

$$F_\beta(t) = \sum_j f_\beta^j \exp(-t/\tau_\beta^j) \quad (8)$$

For the coupled system we assume that the photophysics is

$$F_{\alpha\beta}(t) = \sum_{i,j} f_\alpha^i f_\beta^j F_{\alpha\beta}(t,\tau_\alpha^i,\tau_\beta^j) \quad (9)$$

Here $F_{\alpha\beta}(t,\tau_\alpha^i,\tau_\beta^j)$ is calculated according to eqs 3−5 but with the notation of the lifetimes τ_α^i and τ_β^j instead of τ_α and τ_β, respectively.[11]

Equations 3−9 can be used directly to analyze the fluorescence decay of the $Fl^{2-}-Fl^{1-}$ pair. It is then reasonable to assume that the protolytic reactions are independent of both sides of the lipid-spanning $FlC_{32}Fl$ molecule (see Figure 1). Hereafter the fractions of $Fl^{1-}-Fl^{1-}$, $Fl^{1-}-Fl^{2-}$, and $Fl^{2-}-Fl^{2-}$ pairs are given by $c_{\alpha,in}c_{\alpha,out}$, $(c_{\alpha,in}c_{\beta,out} + c_{\beta,in}c_{\alpha,out})$, and $c_{\beta,in}c_{\beta,out}$, respectively. The fractions of c_α and c_β are given by eq 2. The subscripts "in" and "out" refer to the inner and the outer sides of the vesicles (see Figure 1). Within this formalism the fluorescence decays of FlC_{16} and $FlC_{32}Fl$ are given by

$$F_{16}(t) = (c_{\alpha,in} + c_{\alpha,out})F_\alpha(t) + (c_{\beta,in} + c_{\beta,out})F_\beta(t) \quad (10)$$

and

$$F_{32}(t) = c_{\alpha,in}c_{\alpha,out}F_\alpha(t) + (c_{\alpha,in}c_{\beta,out} + c_{\alpha,in}c_{\beta,out})F_{\alpha\beta}(t) + c_{\beta,in}c_{\beta,out}F_\beta(t) \quad (11)$$

For the analyses of the data we applied eqs 10−11 together with a common deconvolution procedure.[28] Typically two sets of the data were globally analyzed for the fluorescence relaxation of the FlC_{16} and $FlC_{32}Fl$ systems. This required measurements of the fluorescence decays of FlC_{16} and $FlC_{32}Fl$ at similar pH and in the same lipid matrix. In addition to a general improvement of accuracy in a global analysis,[29] this approach was used mainly because it is not possible to directly measure the lifetime of the Fl^{1-}. The monoanion is not dominating at any pH (cf. eq 2). Measurements at very low pH were avoided because of a possible contribution from neutral and other species of fluorescein that would convert to the monoanion upon excitation.[17,18] The quality of the global fitting was judged by standard χ^2 and Durbin−Watson parameters, as well as by the weighted residuals and autocorrelation function plots.

Analyses of the Fluorescence Steady-State Spectra. It is obvious that the excitation and emission spectra of $D_\alpha-D_\beta$ pairs can be described by a linear combination of the individual spectra of D_α and D_β components. Notice, however, that in the presence of energy migration the fractions of these spectral components are no longer directly proportional to the concentrations but depend on the rates $\omega_{\alpha\beta}$ and $\omega_{\beta\alpha}$. Let $p_{ij}(t)$ denote the probability of emission from D_i ($i = \alpha$ or β) at time t provided D_j ($j = \alpha$ or β) was excited at $t = 0$. These probabilities are readily obtained by substituting appropriate $\boldsymbol{p}_{ex}$ and $\boldsymbol{p}_{em}$ into eq 3.[11] For example, one obtains $p_{\alpha\beta}(t)$ by using

$$\boldsymbol{p}_{ex} = \begin{pmatrix} 0 \\ 1 \end{pmatrix}; \qquad \boldsymbol{p}_{em} = \begin{pmatrix} p_{em}^\alpha \\ 0 \end{pmatrix}$$

The steady-state emission of the components in the $D_\alpha-D_\beta$ coupled system are given by

$$I_\alpha^{em} \propto \int_0^\infty [p_{ex}^\alpha p_{\alpha\alpha}(t) + p_{ex}^\beta p_{\alpha\beta}(t)]dt$$

$$I_\beta^{em} \propto \int_0^\infty [p_{ex}^\alpha p_{\beta\alpha}(t) + p_{ex}^\beta p_{\beta\beta}(t)]dt \quad (12)$$

The explicit integration of eqs 12 yields

$$I_\alpha^{em}(\lambda_{ex},\lambda_{em}) \propto \frac{p_{em}^\alpha(\lambda_{em})\tau_\alpha}{1 + \omega_{\alpha\beta}^* + \omega_{\beta\alpha}^*}[p_{ex}^\alpha(\lambda_{ex})(1 + \omega_{\beta\alpha}^*) + p_{ex}^\beta(\lambda_{ex})\omega_{\beta\alpha}^*]$$

$$I_\beta^{em}(\lambda_{ex},\lambda_{em}) \propto \frac{p_{em}^\beta(\lambda_{em})\tau_\beta}{1 + \omega_{\alpha\beta}^* + \omega_{\beta\alpha}^*}[p_{ex}^\beta(\lambda_{ex})(1 + \omega_{\alpha\beta}^*) + p_{ex}^\alpha(\lambda_{ex})\omega_{\alpha\beta}^*] \quad (13)$$

Here λ_{ex} and λ_{em} denotes the excitation and emission wavelength, respectively. For clarity the λ_{ex} and λ_{em} dependence of the fluorescence intensities and probabilities are given. Moreover, $\omega_{\alpha\beta}^* = \tau_\alpha\omega_{\alpha\beta}$ and $\omega_{\beta\alpha}^* = \tau_\beta\omega_{\beta\alpha}$. Note also that $p_{ex}(\lambda_{ex})$ and $p_{em}(\lambda_{em})\tau$ are proportional to the individual excitation

and emission spectra, respectively. Hence, the contributions $x^{\alpha}_{em}(\lambda_{ex})$ and $x^{\beta}_{em}(\lambda_{ex})$ of the D_α and D_β individual emission spectra to the $D_\alpha-D_\beta$ emission spectrum are given by

$$x^{\alpha}_{em}(\lambda_{ex}) \propto p^{\alpha}_{ex}(\lambda_{ex})(1+\omega^{*}_{\beta\alpha}) + p^{\beta}_{ex}(\lambda_{ex})\omega^{*}_{\beta\alpha}$$

$$x^{\beta}_{em}(\lambda_{ex}) \propto p^{\beta}_{ex}(\lambda_{ex})(1+\omega^{*}_{\alpha\beta}) + p^{\alpha}_{ex}(\lambda_{ex})\omega^{*}_{\alpha\beta} \quad (14)$$

Here and in the following, by *contributions* we mean the coefficients in decomposition of the complex spectra, that is $I^{em}_{\alpha\beta} = x^{\alpha}_{em}(\lambda_{ex})I^{em}_{\alpha} + x^{\beta}_{em}(\lambda_{ex})I^{em}_{\beta}$. Note that these coefficients are not necessarily equal to the corresponding fractions of the ionic forms, c_α and c_β.

In an analogous manner expressions for the excitation spectra are obtained as

$$x^{\alpha}_{ex}(\lambda_{em}) \propto p^{\alpha}_{em}(\lambda_{em})(1+\omega^{*}_{\beta\alpha}) + p^{\beta}_{em}(\lambda_{em})\omega^{*}_{\alpha\beta}$$

$$x^{\beta}_{ex}(\lambda_{em}) \propto p^{\beta}_{em}(\lambda_{em})(1+\omega^{*}_{\alpha\beta}) + p^{\alpha}_{em}(\lambda_{em})\omega^{*}_{\beta\alpha} \quad (15)$$

In eqs 14−15 the rates of energy migration (ω^{*}_{ji}/τ_j, $j = \alpha$ or β) depend on the distance between the D_α and D_β groups according to eq 6. The p^{j}_{em} and x^{j}_{ex} functions are determined from decomposition of the steady-state spectra.

In studies of the $FlC_{32}Fl$ system contributions from $Fl^{1-}-Fl^{1-}$ and $Fl^{2-}-Fl^{2-}$ pairs must be considered. For simplicity we consider the case of $pH_{in} = pH_{out}$, for which the total fractions of Fl^{1-} and Fl^{2-} are c_α and c_β, respectively. Then

$$x^{\alpha}_{em}(\lambda_{ex}) \propto \frac{2c_\alpha c_\beta}{1+\omega^{*}_{\alpha\beta}+\omega^{*}_{\beta\alpha}}[p^{\alpha}_{ex}(\lambda_{ex})(1+\omega^{*}_{\beta\alpha}) + p^{\beta}_{ex}(\lambda_{ex})\omega^{*}_{\beta\alpha}] + 2{c_\alpha}^2 p^{\alpha}_{ex}(\lambda_{ex})$$

$$x^{\beta}_{em}(\lambda_{ex}) \propto \frac{2c_\alpha c_\beta}{1+\omega^{*}_{\alpha\beta}+\omega^{*}_{\beta\alpha}}[p^{\beta}_{ex}(\lambda_{ex})(1+\omega^{*}_{\alpha\beta}) + p^{\alpha}_{ex}(\lambda_{ex})\omega^{*}_{\alpha\beta}] + 2{c_\beta}^2 p^{\beta}_{ex}(\lambda_{ex}) \quad (16)$$

or

$$x^{\alpha}_{em}(\lambda_{ex}) \propto p^{\alpha}_{ex}(\lambda_{ex})c_\alpha[c_\alpha(1+\omega^{*}_{\alpha\beta}+\omega^{*}_{\beta\alpha}) + c_\beta(1+\omega^{*}_{\beta\alpha})] + p^{\beta}_{ex}(\lambda_{ex})c_\beta c_\alpha \omega^{*}_{\beta\alpha}$$

$$x^{\beta}_{em}(\lambda_{ex}) \propto p^{\beta}_{ex}(\lambda_{ex})c_\beta[c_\beta(1+\omega^{*}_{\alpha\beta}+\omega^{*}_{\beta\alpha}) + c_\alpha(1+\omega^{*}_{\alpha\beta})] + p^{\alpha}_{ex}(\lambda_{ex})c_\alpha c_\beta \omega^{*}_{\alpha\beta} \quad (17)$$

The corresponding expressions for the excitation spectra are

$$x^{\alpha}_{ex}(\lambda_{em}) \propto p^{\alpha}_{em}(\lambda_{em})c_\alpha[c_\alpha(1+\omega^{*}_{\alpha\beta}+\omega^{*}_{\beta\alpha}) + c_\beta(1+\omega^{*}_{\beta\alpha})] + p^{\beta}_{em}(\lambda_{em})c_\beta c_\alpha \omega^{*}_{\alpha\beta}$$

$$x^{\beta}_{ex}(\lambda_{em}) \propto p^{\beta}_{em}(\lambda_{em})c_\beta[c_\beta(1+\omega^{*}_{\alpha\beta}+\omega^{*}_{\beta\alpha}) + c_\alpha(1+\omega^{*}_{\alpha\beta})] + p^{\alpha}_{em}(\lambda_{em})c_\alpha c_\beta \omega^{*}_{\beta\alpha} \quad (18)$$

Results and Discussion

Properties of Fluorescein in Lipid Bilayers. To calculate the excitation and emission probabilities (eq 5) and the Förster radii (eq 7), we need to know the absorption and fluorescence spectra of Fl^{1-} and Fl^{2-}. These spectra were recovered from experimental data by using two different approaches.[25,26] In the first approach one assumes a model for the ionization of fluorescein, which is then used in fitting to experimental results. This procedure provides the individual spectra of Fl^{1-} and Fl^{2-} and the pK_a values, as described elsewhere.[25] For FlC_{16} and $FlC_{32}Fl$ solubilized in lipid bilayers, the ionization model of fluorescein in water (i.e., eq 1) would be appropriate, because the chemical modifications of fluorescein (Figure 1) have a negligible affect on the ionisable groups. Furthermore, the polar fluorescein group is exposed to water in the bilayer interface.[30]

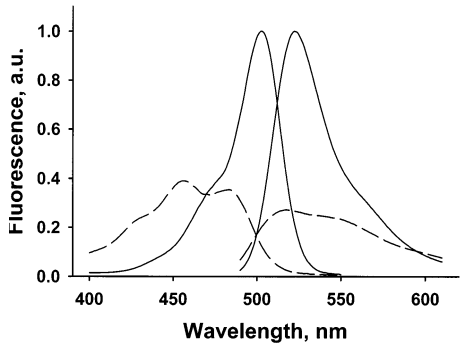

Figure 2. Emission and excitation spectra of Fl^{2-} (solid lines) and Fl^{1-} (dashed lines). The spectra were obtained for the FlC_{16} molecule solubilized in the DOPC bilayer at 22 °C. For this system the pK_a of the monoanion−dianion transition (pK_2) is found to be 8.0.

Here all measurements were performed at pH > 7.5 (vide infra) at which the simplified model (eq 1) appeared justified, as judged from the absence of any systematic deviation between calculated and experimental data.

To calculate the pK_a values the fluorescence spectra were analyzed for FlC_{16} solubilized in DOPC vesicles at six different pH values ranging from 5.76 to 8.57. From the set of excitation spectra, we extracted values of $pK_1 = 5.9$ and $pK_2 = 8.0$. These values are significantly higher than those of fluorescein in aqueous solution (4.31 and 6.43, respectively).[17] An apparent reason for this difference is the localization of the fluorescein groups in the lipid−water interface with its local heterogeneity in physicochemical properties.[31] For a difference of 2.1 between the two pK_a values one can for $pH \cong pK_2$ ignore ionic forms other than those considered in eq 1.

The light scattering caused by the vesicles perturbs the analysis of the absorption spectra. To reduce scattering, absorption spectra were studied for the fluorescein probes solubilized in micelles of lyso-PPC. Although the lipid−water interface regions are chemically very similar, the pK_a values need not be exactly the same for the micellar and vesicle systems. Therefore, only the maximum molar absorptivity of Fl^{1-} was calculated from the absorption spectra, which would otherwise be difficult to obtain. It was found to be 30 000 M^{-1} cm^{-1}, provided that the molar absorptivity of the dianion is 76 900 M^{-1} cm^{-1}.[17] The former value is very similar to the value of 29 000 M^{-1} cm^{-1} in water, previously reported.[17] For the dianion the values of 68 000[12] and 88 000 M^{-1} cm^{-1} [18] were also reported. These molar absorptivites were used only to calculate the Förster radii (eq 7) of which the uncertainty means a potential error within 2.5%.

A second approach for calculating the individual spectral components would be to measure two-dimensional spectra which are then analyzed by the DATAN method[26] or by any other appropriate algorithm.[32] The spectra thus found by DATAN are displayed in Figure 2. In fact, the spectra are very similar to those found as described above using the model given by eq 1,

TABLE 1: The Förster Radii for Different Combinations of Mono- (Fl^{1-}) and Dianionic (Fl^{2-}) Forms of Fluorescein[a]

ionic form	R_0, acceptor = Fl^{2-}	R_0, acceptor = Fl^{1-}	τ, ns	Φ
Fl^{2-}	48.9 ± 1.3	33.5 ± 0.9	4.1 ± 0.1	0.88 ± 0.02
Fl^{1-}	43.3 ± 1.6	30.9 ± 1.1	4.7 ± 0.3[b]	0.41 ± 0.03

[a] The fluorescence quantum yields (Φ) and lifetimes (τ) are also given. The data were obtained for FlC_{16} solubilized in bilayers of DOPC. [b] The average lifetime found in global analysis. The fluorescence decay of Fl^{1-} was biexponential.

which supports eq 1. The shapes of the spectra are similar to those in aqueous solution,[17,18] although maxima are slightly shifted. The monoanion and dianion of fluorescein exhibit absorption maxima at 465 and 503 nm and fluorescence maxima at 518 and 522 nm, respectively.

The fluorescence quantum yields of Fl^{2-} and Fl^{1-} were obtained to be 0.88 ± 0.02 and 0.41 ± 0.03, respectively. The quantum yield of Fl^{2-} was measured at pH ≅ 10, while that for Fl^{1-} was calculated using the integrals of the Fl^{1-} and Fl^{2-} emission spectra previously determined for the pH range 5.76−8.57. For Fl^{2-} Magde et al.[33] have reported a quantum yield of 0.90 ± 0.02. The Förster radii calculated according to eq 7 together with other photophysical properties are collected in Table 1.

Time-Resolved Experiments and Data Analysis. The fluorescence lifetime measurements of $Fl^{2-}-Fl^{2-}$ and $Fl^{1-}-Fl^{1-}$ pairs contain no information about the rates of energy migration.[3] Therefore, it is desirable to keep the fractions of these pairs relatively small, as compared to $Fl^{2-}-Fl^{1-}$ pair. This corresponds to an optimum pH value of about pK_2 (cf. eq 2) provided that $pH_{in} = pH_{out}$. The creation of a transmembrane pH gradient provides another way to increase the fraction of the $Fl^{2-}-Fl^{1-}$ pairs (vide infra).

By a rational choice of the excitation and emission wavelengths it is also possible to increase the contribution from $Fl^{2-}-Fl^{1-}$ pairs to the observed fluorescence. A ratio of $p^{\beta}_{ex}/p^{\alpha}_{ex} = 0.38$ at the peak excitation wavelength of 450 nm was calculated from the overlap between the spectral distribution density of the light source and the excitation spectra. To estimate the emission probability ratio is not a straightforward task because it depends on properties of the detection system. Here we estimated $p^{\beta}_{em}/p^{\alpha}_{em}$ from the overlap between the emission spectra and the transmission of the emission filter or monochromator. A ratio of $p^{\beta}_{em}/p^{\alpha}_{em} \cong 2.3$ was found at the emission wavelength of 550 nm. However, using this value in the analysis as a fixed parameter usually provided poor fitting to data. Therefore, we considered the $\boldsymbol{p}_{em}$ vector (or more precisely, the $p^{\beta}_{em}/p^{\alpha}_{em}$ ratio) as a floating parameter in the analysis and found acceptable statistical criteria. In previous work we ascertained that the accuracy of the distance determination is slightly worse when $\boldsymbol{p}_{ex}$ and $\boldsymbol{p}_{em}$ are floating,[11] although the accuracy was acceptable. The $\boldsymbol{p}_{em}$ values extracted were always compared and found to agree with the value given above, as well as with the values obtained by repeating the experiments several times. The statistics was not further improved for floating $\boldsymbol{p}_{ex}$ values, but scatter of the R values increased.

$FlC_{32}Fl$ Solubilized in DOPC Vesicles. In a series of experiments we examined $FlC_{32}Fl$ solubilized in DOPC vesicles at $pH_{in} = pH_{out} \approx pK_2$. Figure 3 displays the fluorescence decay of $FlC_{32}Fl$. Although the decay might seem very similar to that of FlC_{16}, one should notice the shift of the peak of the $FlC_{32}Fl$ decay, while the curves are almost parallel at times after the excitation pulse. This is strongly indicative of energy transfer,

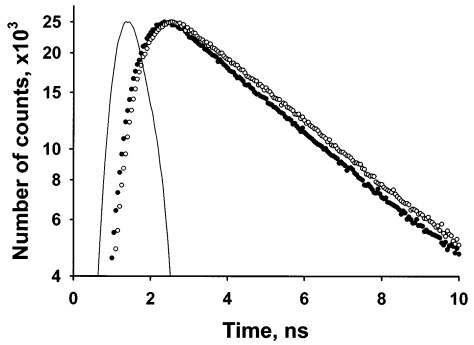

Figure 3. Fluorescence decay curves obtained for FlC_{16} (solid circles) and $FlC_{32}Fl$ (open circles) in DOPC vesicles. The response function is also shown (solid line). The distance between Fl fluorophores calculated from the shown data is 39.9 Å.

preferably in the direction of $Fl^{1-} \rightarrow Fl^{2-}$. From a fitting of the PDDEM model (eqs 3−11) to experimental decays, we determine a distance of 39.2 ± 1.6 Å (see Table 2) between the fluorescein groups. The $\langle\kappa^2\rangle$ factor appearing in eq 6 was estimated from the time-resolved depolarization data as described elsewhere.[3] The $\langle\kappa^2\rangle$ values obtained for different pH range between of 0.46−0.49, which is close to $\langle\kappa^2\rangle \cong 0.45$ found for a rhodamine dye of similar structure.[8,34] The $p^{\beta}_{em}/p^{\alpha}_{em}$ value is 1.67 ± 0.14 that is somewhat lower than the calculated value.

The distance obtained between the Fl moieties agrees with thickness of a DOPC bilayer (∼38 Å) that was previously determined by X-ray diffraction.[35] Our results are also comparable with studies by Kachel et al.,[30] where the location of different fluorophores in lipid bilayers was investigated. They found that fluorescein is located at 20.5−23.5 Å from the center of DOPC bilayers (at pH 10). Taking into account the slightly different structures of our probes and the rather high pH, these data are also in a reasonable agreement with our results. Finally, we measured the distance between Fl^{2-} fluorophores using the DDEM method. This experiment was performed at pH 10.3, for which the dianionic form is dominating. The distance obtained from DDEM experiment is 38.6 Å (Table 2). Moreover, no significant difference between the lifetimes of FlC_{16} and $FlC_{32}Fl$ was observed in the DDEM experiment, indicating that close contact between Fl groups is improbable.[8,36] Thus, we conclude that $FlC_{32}Fl$ strongly prefers the transbilayer conformation and the contribution from bent $FlC_{32}Fl$ molecules to the fluorescence is negligible.[8] The conformation of a rhodamine dye of very similar structure is discussed in refs 8 and 34.

To explore the sensitivity of the statistical parameters to various R values obtained by global analyses of FlC_{16} and $FlC_{32}Fl$, the following tests were performed. The distances (R') were fixed at the values of 1.1R and 0.9R, while other floating parameters in the analysis were kept free, as before. The average χ^2 value corresponding to both $R' = 1.1R$ and $R' = 0.9R$ was 1.23, which is significantly higher than the χ^2 found for the correct distance R. The χ^2 parameter corresponding to the fluorescence relaxation of FlC_{16} was typically slightly higher for distances forced to be R'. Some of the fitting results were also rejected because negative p_{em} values were extracted.

Analyses of Synthetically Generated Data. The small difference between the fluorescence decays of FlC_{16} and $FlC_{32}Fl$ (see Figure 3) raises the question: How reliable is a distance determination? By using the experimental lifetimes of Fl^{1-} and Fl^{2-} at $pH_{in} = pH_{out} = pK_2 = 8$ and for the Förster radii of 43.3 Å ($Fl^{1-} \rightarrow Fl^{2-}$) and 33.4 Å ($Fl^{2-} \rightarrow Fl^{1-}$) synthetic data were generated for distances ranging between 20 and 60 Å. For each distance, 10 independent "experiments" were generated,

TABLE 2: Distance (R) between Fluorescein Groups of $FlC_{32}Fl$ Molecule Solubilized in Lipid Bilayers of DOPC and DMPC[a]

system	method	R, Å	average χ^2	$p^{\beta}_{em}/p^{\alpha}_{em}$	τ_α, ns [b]
DOPC, pH ≈ pK_2	PDDEM	39.2 ± 1.6	1.11	1.67 ± 0.14	4.7 ± 0.3
DOPC, pH ≫ pK_2	DDEM	38.6	1.05[c]		
DMPC, pH ≈ pK_2	PDDEM	34.0 ± 1.0	1.06	1.85 ± 0.14	4.5 ± 0.2
DMPC, pH ≫ pK_2	DDEM	34.8	1.14[c]		
DOPC, $pH_{in} < pH_{out}$[d]	PDDEM	40.2 ± 0.9	1.19	3.33 ± 0.86	5.3 ± 0.8
DOPC, pH ≈ pK_2	2DSSF	40.2 ± 1.3			

[a] The results are obtained from the analyses of time-resolved and steady-state experiments that were analyzed according to the DDEM, PDDEM and 2-dimensional steady-state fluorescence (2DSSF) methods. [b] The average lifetime. [c] The average χ^2 values presented for the DDEM experiments correspond to the difference curves. [d] pH gradient of about 1 unit was created in this system.

and the average error for each distance was calculated. The errors are typically less than 3% for distances between 27 and 60 Å. To investigate the influence of an uncertainty in the pK_2 value, a true value of 7.8 was assumed in the simulations of synthetic data, while we forced it to be 8.0 in the analyses. This introduces a systematic error over the entire range of distances, so that slightly shorter distances are expected as compared to the true values. However the error is less than 2%.

$FlC_{32}Fl$ Solubilized in DMPC Vesicles. $FlC_{32}Fl$ solubilized in DMPC vesicles was studied in another series of experiments. To avoid lipid bilayers in the gel state, temperature was increased to 303 K. Except for temperature, the experimental conditions were the same as for the DOPC system. The average distance between Fl^{1-} and Fl^{2-} calculated from the fluorescence relaxation of $FlC_{32}Fl$ is 34.0 ± 1.0 Å (Table 2), which is in excellent agreement with the thickness of 34.5 Å obtained from X-ray diffraction.[37] The $p^{\beta}_{em}/p^{\alpha}_{em}$ value of 1.85 ± 0.14 is similar to that found for DOPC. In this case, however, the stability of the analysis was worse. The average value of χ^2 was 1.13 and 1.09 for fixed distances of $R' = 1.1R$ and $R' = 0.9R$, respectively. It means that $\chi^2(R)$ exhibits a flat minimum that implies less stable analyses. In fact such instabilities were predicted in previous work of the accuracy of re-analyzing PDDEM data obtained from simulated TCSPC experiments.[11] Nevertheless, a minor scattering in distance (± 1.0 Å, Table 2) suggests that sufficient information about the energy migration rates is still contained in fluorescence relaxation of $FlC_{32}Fl$. In this context one should also note that the distance between the fluorescein groups of $FlC_{32}Fl$ in DMPC bilayer also agrees with that obtained from DDEM experiment (Table 2).

Vesicles with a Transbilayer pH Gradient. By creating a transmembrane pH gradient it is possible to increase the fraction of $Fl^{2-}-Fl^{1-}$ pairs. For example, this fraction is at the most 0.50 when $pH_{in} = pH_{out}$, while it is 0.78 for $pH_{in} = 7$ and $pH_{out} = 9$ (eq 2). We therefore created a pH gradient by adding sodium hydroxide to a vesicle suspension, whereby one expects to obtain data of a better quality. In practice the creation a pH gradient involves several difficulties. At first, we estimated the rate of proton leakage from DOPC vesicles that were loaded with pyranine. This procedure is described elsewhere.[22] The leakage turned out to be slow (less than 0.05 pH units during the experiment) below 283 K. Consequently, all pH gradient experiments were performed at this temperature. However, we observed a small, rapid rise in pH_{in} immediately after addition of a base aliquot, which we cannot clearly explain. It is important that the nontrapped dye molecules were for sure not the reason. The initial jump of pH_{in} was about 0.2, while pH_{out} was increased by about 1 unit. In further analysis of the data this deviation was accounted for.

The R values obtained for the system with a pH gradient are presented in Table 2. One should notice that the $p^{\beta}_{em}/p^{\alpha}_{em}$ value is significantly higher than that found for the DOPC and DMPC vesicles. Also, the average value of χ^2 of 1.19 is relatively high. This may indicate errors in estimating the fractions of Fl^{1-} and Fl^{2-} (i.e., eq 2 used in eqs 10−11) caused by uncertainties in pH_{in}. Nevertheless, a reasonable distance was determined, as is shown in Table 2. As it appears, the lifetimes of $FlC_{32}Fl$ contain the main information about the energy migration rates, rather than the preexponential factors that depend on $\boldsymbol{p}_{em}$ and pH_{in}. This is compatible with the fact that all preexponential factors can be floating in the PDDEM data analysis, as was previously shown.[11] The somewhat long lifetime of Fl^{1-} (Table 2) found in global analysis is reasonable because of the rather low temperature of the experiments. Average χ^2 values of 1.25 and 1.33 were obtained when the distance was fixed at the values of $1.1R$ and $0.9R$, respectively.

Fluorescence Steady-State Experiments and Two-Dimensional Analysis. The steady-state spectra recorded for $FlC_{32}Fl$ solubilized in lipid vesicles can be used to calculate the rates of energy migration (eqs 17−18). Interestingly it turns out that the distance R is the only fitting parameter needed for the analysis. Except for the lifetimes, all other parameters appearing in eqs 17−18 can be calculated from the steady-state data. We here show how to extract the migration rates from the two-dimensional (2D) fluorescence spectra of FlC_{16} and $FlC_{32}Fl$. Each spectrum in a set can be decomposed to obtain the contributions of Fl^{1-} and Fl^{2-} spectra $x_{ex}(\lambda_{em})$ or $x_{em}(\lambda_{ex})$. The fractions of the ionic forms c_α and c_β was calculated according to eq 2. Thus, one obtains all parameters in eq 18 except for the rates, which depend on the distance R according to eq 6.

To test the steady-state model we used $FlC_{32}Fl$ solubilized in DOPC vesicles at $pH_{in} = pH_{out} \cong pK_2$. At first the 2D spectra of FlC_{16} were recorded under similar conditions. In practice we decomposed only the excitation spectra, because the components (i.e., the excitation spectra of Fl^{1-} and Fl^{2-}) provide the best separation (cf. Figure 2). It means that a complex excitation spectrum can be resolved with better precision. Thus, each excitation spectrum from the set was resolved into the Fl^{1-} and Fl^{2-} spectra obtained before (Figure 2). The contributions of these spectra are $p^{\alpha}_{em}(\lambda_{em})c_\alpha$ and $p^{\beta}_{em}(\lambda_{em})c_\beta$, respectively (cf. eq 18, $\omega^*_{\alpha\beta} = \omega^*_{\beta\alpha} = 0$). Then the excitation spectra of $FlC_{32}Fl$ were resolved in the same way to obtain $x^{\alpha}_{ex}(\lambda_{em})$ and $x^{\beta}_{ex}(\lambda_{em})$ in eq 18. The contribution of the Fl^{2-} excitation spectrum in the spectra of FlC_{16} and $FlC_{32}Fl$ is shown in Figure 4. The data points corresponding to the $FlC_{32}Fl$ spectra contain a larger fraction of the Fl^{1-} spectrum, compatible with a fraction of Fl^{2-}excited indirectly by energy transfer from Fl^{1-}. By fitting eq 18 to the data yields the distance of 40.2 ± 1.3 Å (Table 2), which actually agrees very well with the values reported above. The solid line in Figure 4 represents the best fit corresponding to the distance found. The curves calculated using the wrong distances $R' = 0.9R$ and $1.1R$ are clearly below and above the data points, respectively (Figure 4, dashed lines). The corresponding mean square deviations are 3 to 8 times higher for the wrong distances than for R.

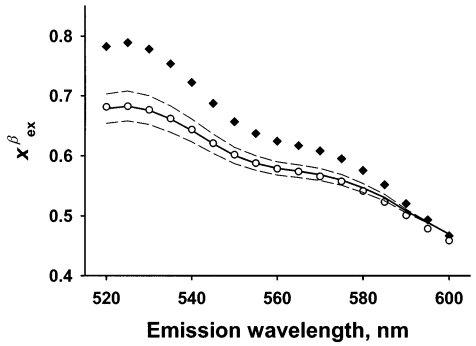

Figure 4. Contribution of Fl^{2-} to the excitation spectra is shown as a function of the emission wavelength. The data for FlC_{16} (solid diamonds) and $FlC_{32}Fl$ (open circles) are shown. The best fit to the $FlC_{32}Fl$ data (solid line) corresponds to a distance $R = 41.1$ Å. The theoretical curves calculated using $R' = 0.9R$ and $1.1R$ (dashed lines) are below and above the best fit, respectively.

Concluding Remarks

Partial donor−donor energy migration can be used for distance measurements within pairs of fluorescent groups of the same kind, which reside in anisotropic systems such as lipid membranes. A prerequisite is that interacting fluorophores respond to different physicochemical environments. The response may be spectral shifts caused by polarity, chemical equilibria between different forms of the fluorophore (e.g. caused by pH, as in the present work), or a different quenching. Quenching seems attractive in studies of proteins, for which different positions of the structure may be differently accessible to a quencher. To exemplify consider the BODIPY group, which is rather inert to solvent polarity and pH.[9,10] However, the BODIPY fluorophore is quenched by I^- (M. Isaksson, 2002, unpublished data) enabling different photophysics between two positions in a protein structure, and thereby information about distances. Sulfhydryl specific derivatives of BODIPY can be specifically linked to a Cys residue of a protein. By means of site-specific *mutagenesis* Cys can often replace or be replaced in a protein, as is exemplified in previous work.[38] In current research we are using this approach to test the PDDEM method as well as examine the plasminogen activator inhibitor type 2. Preliminary results provide further for the PDDEM method.

Acknowledgment. The Swedish Research Council, the Kempe Foundations and the Russian Foundation for Basic Research have financially supported this work.

References and Notes

(1) Van der Meer, B. W.; Coker, G., III; Chen, S.-Y. S. *Resonance Energy Transfer: Theory and Data*; VCH Publishers: New York, 1994.

(2) Lakowicz, J. R. *Principles of Fluorescence Spectroscopy*, 2nd ed.; Kluwer Academic/Plenum Publishers: New York:, 1999.

(3) Johansson, L. B.-Å.; Bergström, F.; Edman, P.; Grechishnikova, I. V.; Molotkovsky, J. G. *J. Chem. Soc., Faraday Trans.* **1996**, *92*, 1563−1567.

(4) Karolin, J.; Fa, M.; Wilczynska, M.; Ny, T.; Johansson, L. B.-Å. *Biophys. J.* **1998**, *74*, 11−21.

(5) Bergström, F.; Hägglöf, P.; Karolin, J.; Ny, T.; Johansson, L. B.-Å. *Proc. Natl. Acad. Sci. U.S.A.* **1999**, *96*, 12477−12481.

(6) Wilczynska, M.; Fa, M.; Karolin, J.; Ohlsson, P.-I.; Johansson, L. B.-Å.; Ny, T. *Nat. Struct. Biol.* **1997**, *4*, 354−356.

(7) Fa, M.; Bergström, F.; Hägglöf, P.; Wilczynska, M.; Johansson, L. B.-Å.; Ny, T. *Structure* **2000**, *8*, 397−405.

(8) Karolin, J.; Bogen, S.-T.; Johansson, L. B.-Å.; Molotkovsky, J. G. *J. Fluoresc.* **1995**, *5*, 279.

(9) Karolin, J.; Johansson, L. B.-Å.; Strandberg, L.; Ny, T. *J. Am. Chem. Soc.* **1994**, *116*, 7801−7806.

(10) Bergström, F.; Mikhalyov, I.; Hägglöf, P.; Wortmann, R.; Ny, T.; Johansson, L. B.-Å. *J. Am. Chem. Soc.* **2002**, *124*, 196−204.

(11) Kalinin, S. V.; Molotkovsky, J. G.; Johansson, L. B.-Å. *Spectrochim. Acta, Part A* **2002**, *58*, 1087−1097.

(12) Haugland, R. P. *Handbook of Fluorescent Probes and Research Chemicals*, 6th ed.; Molecular Probes: Eugene, OR, 1996.

(13) Galla, H. J.; Sackmann, E. *J. Am. Chem. Soc.* **1975**, *97*, 4114−4120.

(14) Lentz, B. R.; Barenholz, Y.; Thompson, P. E. *Biochemistry* **1976**, *15*, 4521−4528.

(15) Hutterer, R.; Parusel, A. B. J.; Hof, M. *J. Fluoresc.* **1998**, *8*, 389−393.

(16) Struck, D. K.; Hoekstra, D.; Pagano, R. E. *Biochemistry* **1981**, *20*, 4093−4099.

(17) Sjoback, R.; Nygren, J.; Kubista, M. *Spectrochim. Acta A* **1995**, *51*, L7−L21.

(18) Klonis, N.; Sawyer, W. H. *J. Fluoresc.* **1996**, *6*, 147−157.

(19) Johansson, L. B.-Å.; Kalinin, S. V.; Filatova, K. A.; Molotkovsky, J. G. *Russ. J. Bioorg. Chem.* **2003**, *29*, 80−84.

(20) Grechishnikova, I. V.; Johansson, L. B.-Å.; Molotkovsky, J. G. *Chem. Phys. Lipids* **1996**, *81*, 87−98.

(21) Hope, M. Y.; Bally, M. B.; Cullis, P. R. *Biochim. Biophys. Acta* **1985**, *812*, 55.

(22) Kamp, F.; Hamilton, J. A. *Proc. Natl. Acad. Sci. U.S.A.* **1992**, *89*, 11367−11370.

(23) Kalinin, S.; Speckbacher, M.; Langhals, H.; Johansson, L. B.-Å. *Phys. Chem. Chem. Phys.* **2001**, *3*, 172−174.

(24) Chowdhury, F. N.; Kolber, Z. S.; Barkley, M. D. *Rev. Sci. Intrum.* **1991**, *62*, 47.

(25) Kubista, M.; Sjoback, R.; Nygren, J. *Anal. Chim. Acta* **1995**, *302*, 121−125.

(26) Scarminio, I.; Kubista, M. *Anal. Chem.* **1993**, *65*, 409−416.

(27) Förster, T. *Ann. Phys.* **1948**, *2*, 55−75.

(28) O'Connor, D. V.; Phillips, D. *Time-correlated Single Photon Counting*; Academic Press: London, 1984.

(29) Knutson, J. R.; Beechem, J. M.; Brand, L. *Chem. Phys. Lett.* **1983**, *102*, 501−507.

(30) Kachel, K.; Asuncion-Punzalan, E.; London, E. *Biochim. Biophys. Acta* **1998**, *1374*, 63−76.

(31) Tocanne, J. F.; Teissie, J. *Biochim. Biophys. Acta* **1990**, *1031*, 111−142.

(32) Bro, R. *Chemom. Intell. Lab. Syst.* **1997**, *38*, 149−171.

(33) Magde, D.; Wong, R.; Seybold, P. D. *Photochem. Photobiol.* **2002**, *75*, 327−334.

(34) Bogen, S.-T.; Karolin, J.; Molotkovsky, J. G.; Johansson, L. B.-Å. *J. Chem. Soc., Faraday Trans.* **1998**, *94*, 2435−2440.

(35) Bergenståhl, A. B.; Stenius, P. *J. Phys. Chem.* **1987**, *81*, 5944.

(36) Runnels, L. W.; Scarlata, S. F. *Biophys. J.* **1995**, *69*, 1569−83.

(37) Lis, L. J.; McAlister, M.; Fuller, N.; Rand, R. P.; Parsegian., V. A. *Biophys. J.* **1982**, *37*, 657−665.

(38) Fa, M.; Karolin, J.; Aleshkov, S.; Strandberg, L.; Johansson, L. B.-Å.; Ny, T. *Biochemistry* **1995**, *24*, 13833−13840.